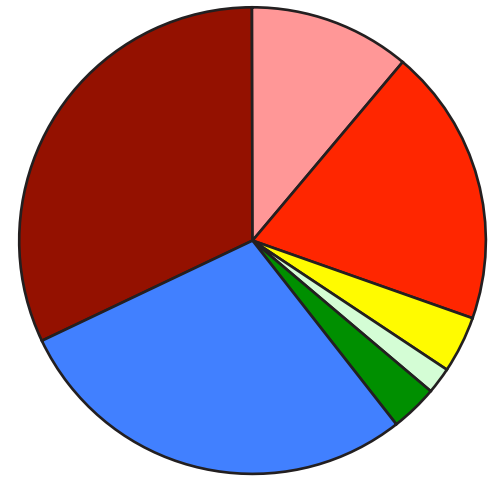
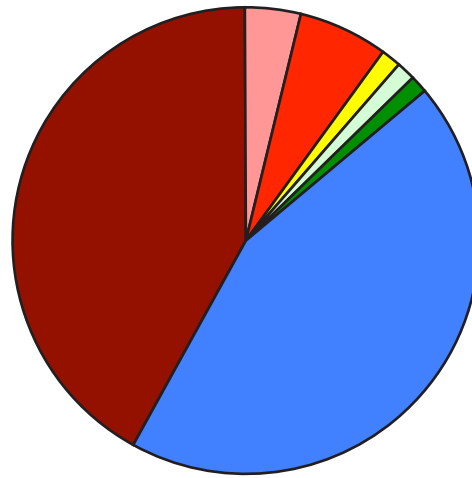
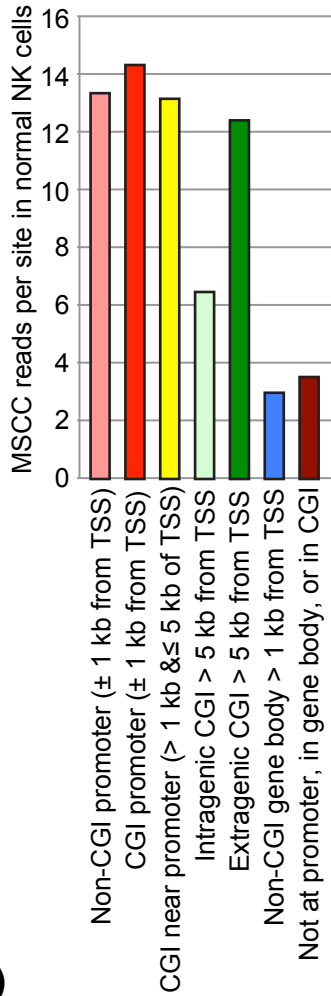


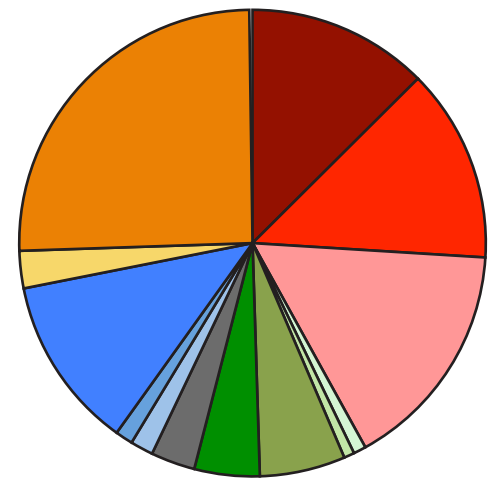
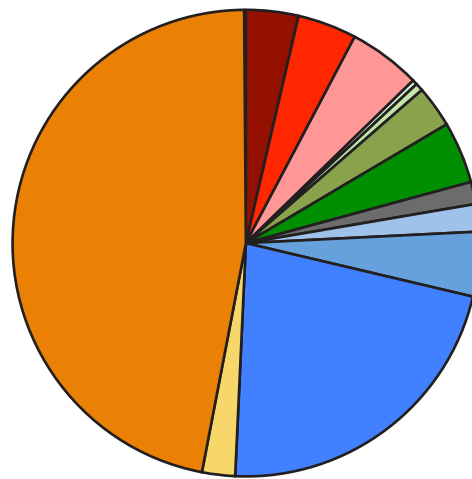
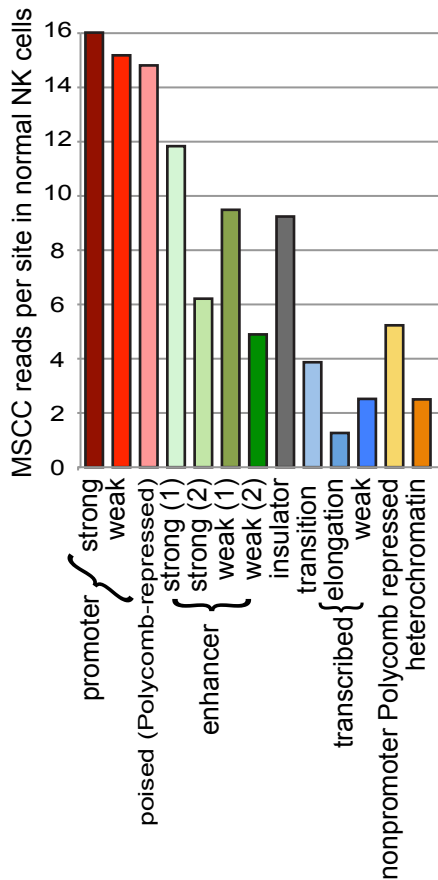
Figure S1

Distribution of MSCC Cut Sites

A)



B)



Mappable HpaII sites were divided into categories based on either **(A)** their position within the promoter region or gene body and within a CGI or **(B)** the chromatin structure of the adjacent DNA in hESCs, as described in the text. For each classification, the left panel shows the average number of reads per site in normal NK cells for each category (average of 3 technical replicates); the middle panel shows the distribution of sites among the various categories; and the right panel shows in distribution of reads among the categories in normal NK cells. Colors are coded as in Fig. 1.

Figure S2. Mean log₂ cut counts per site for promoters and bodies of genes with differing normal NK expression levels

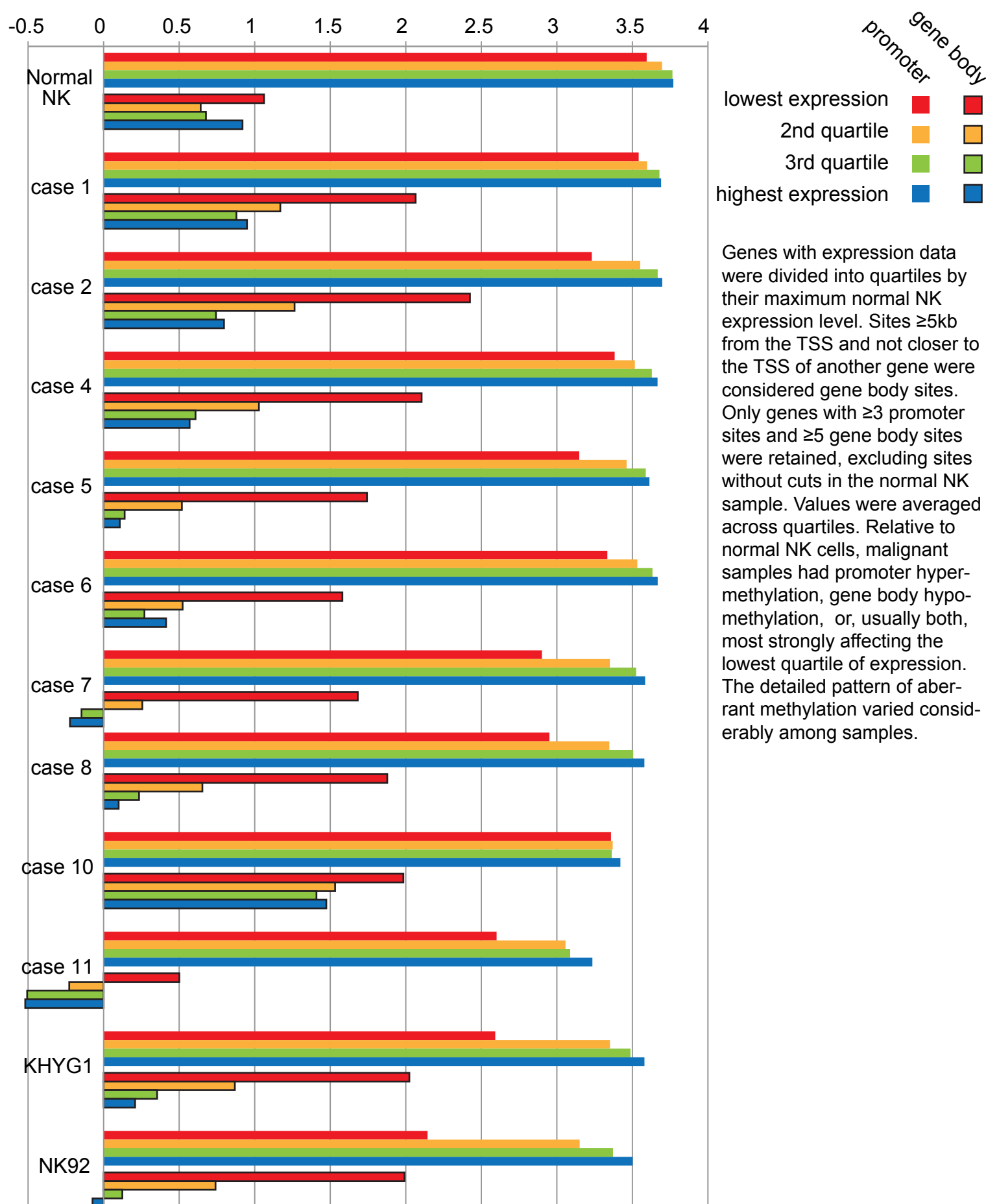
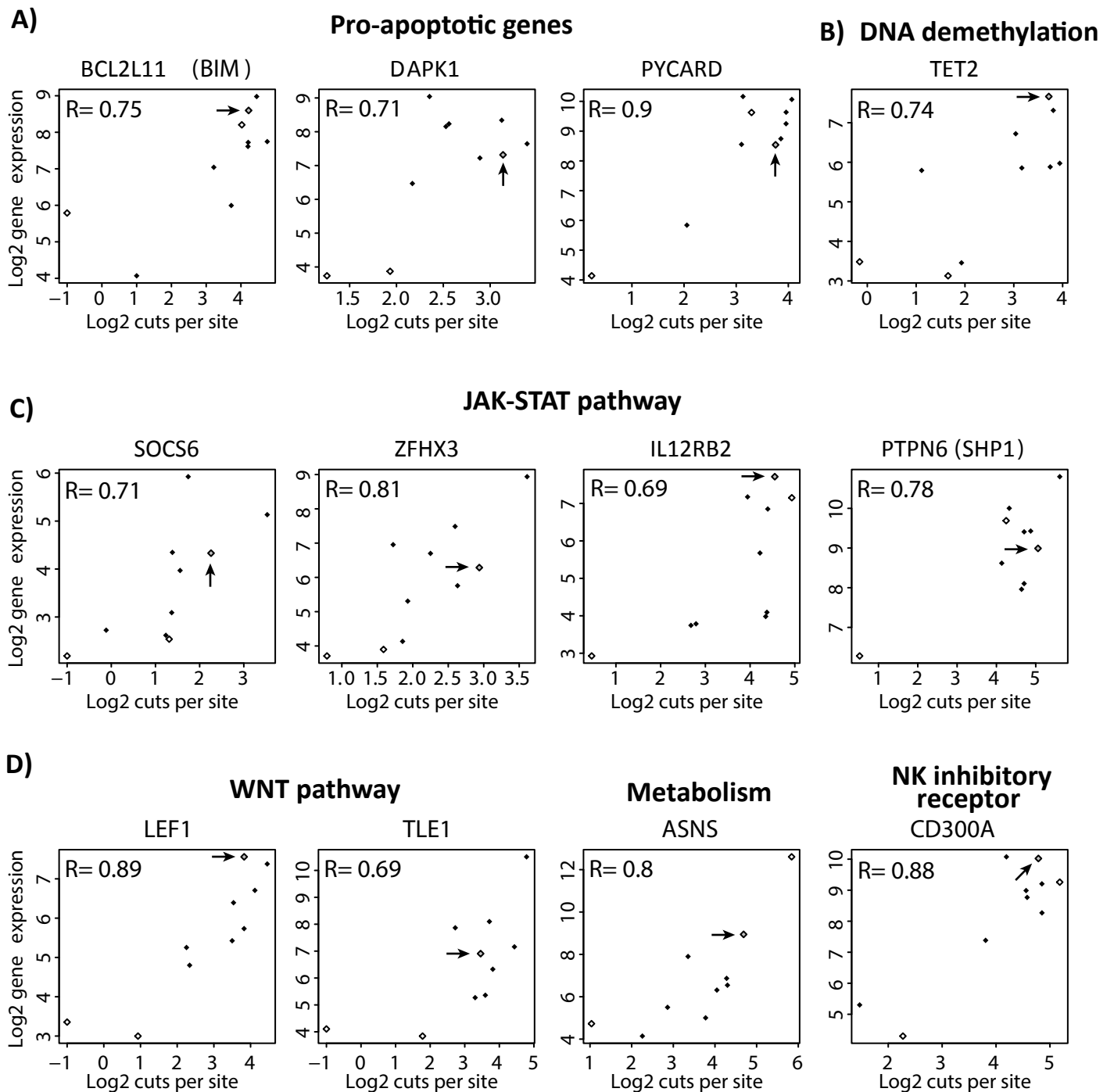


Figure S3



Correlation of promoter hypermethylation and gene expression of candidate genes in malignant NK samples. The total number of MSCC cut sites within 1 kb from the TSS for pro-apoptotic genes (A), DNA-methylation modifiers (B), negative regulators of JAK-STAT signaling pathway (C), WNT pathway, metabolic pathway, and NK-cell activation-associated genes (D) was summed for each malignant (n=9) or normal NK sample (average of 3 technical replicates) and compared with the HG U133Plus2 gene expression values for the corresponding sample to show the correlation between low promoter cut counts (i.e. hypermethylation) and low gene expression values using scatter plots. Pearson correlation coefficients (R) between MSCC cut count and gene expression values are shown in each plot. The point representing the mean MSCC and GEP values for normal NK cells is indicated by an arrow and shown in gray. Two NK-cell lines are shown as white filled diamond shapes to differentiate them from NKCL cases, which are shown as black diamond shapes. Plots show log₂ converted values of MSCC cut counts or DNA microarray gene expression values.

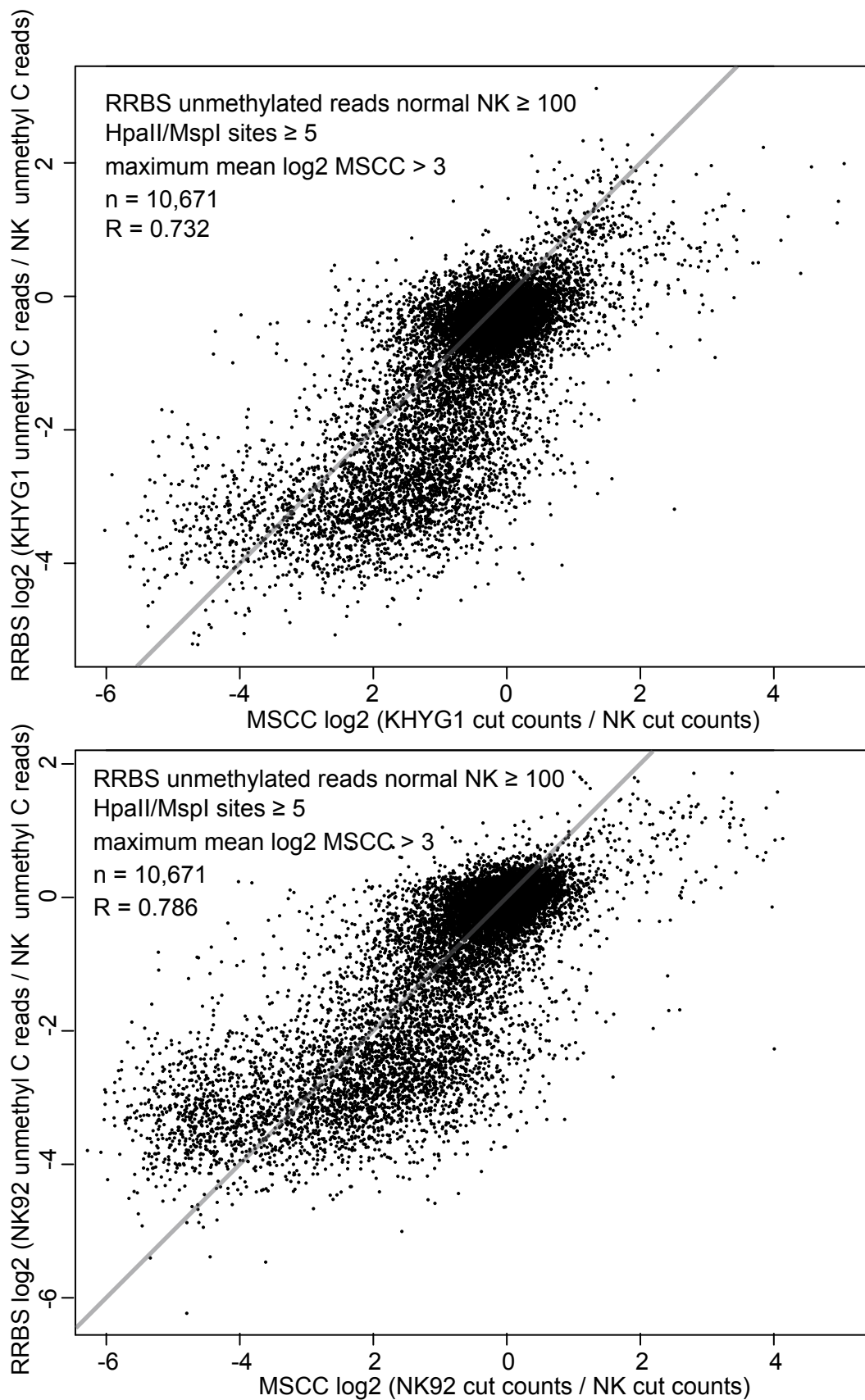
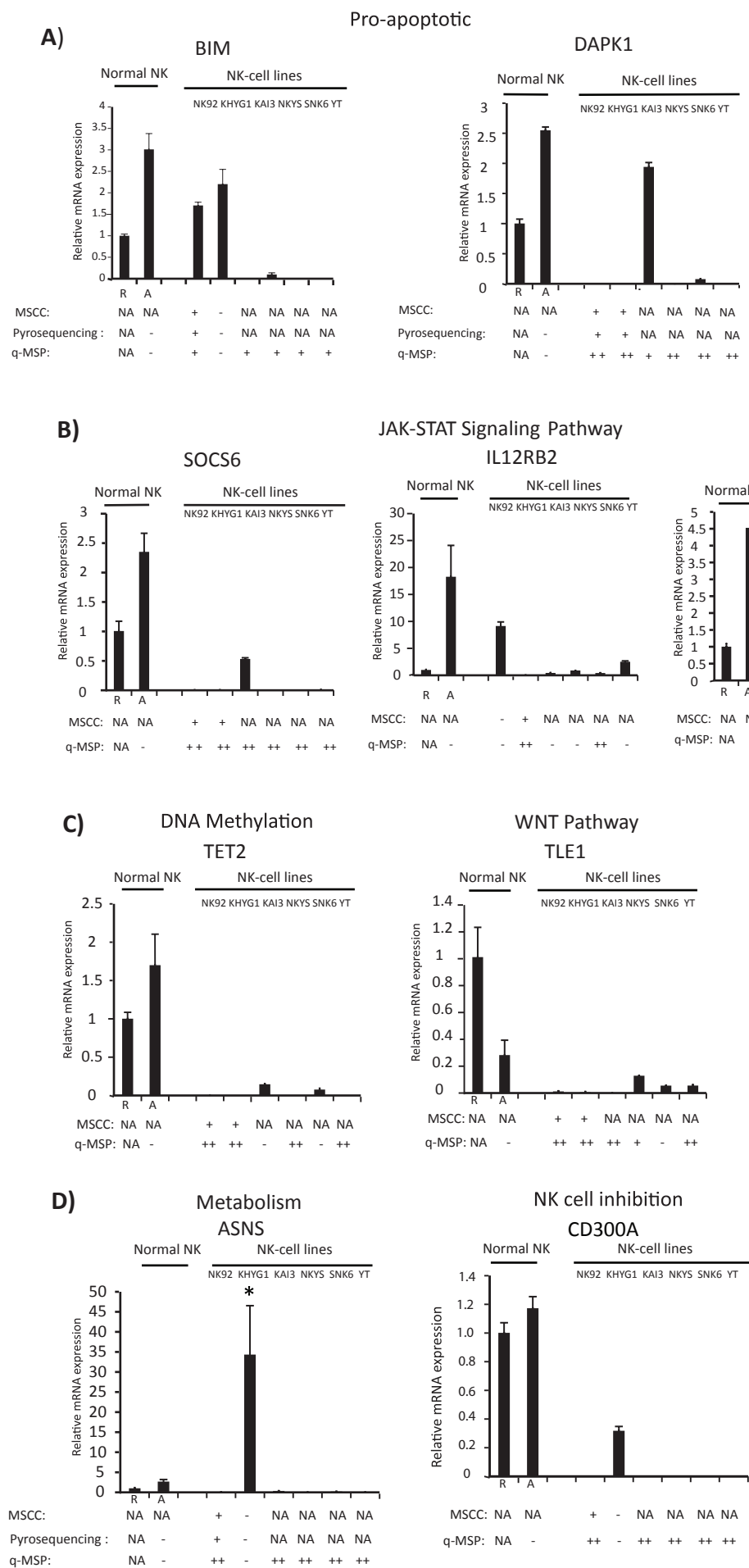


Figure S4. Genome-wide comparisons of MSCC and RRBS methodologies on detection of promoter methylation levels.

All unmethylated RRBS reads at CpGs \pm 1 kb of the TSS were summed for each gene.

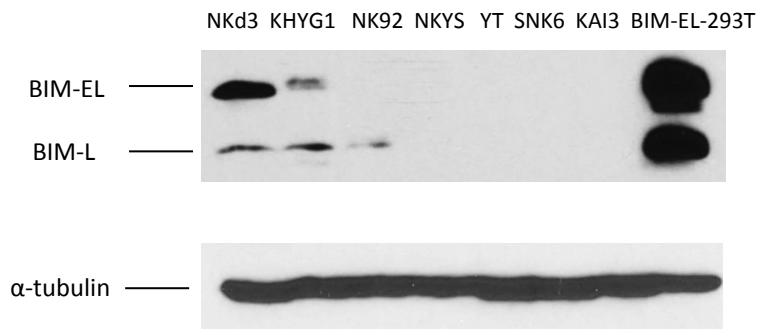
For each of 10,671 genes that pass the three indicated filters, the log₂ change from normal, as assessed by MSCC, was plotted against the corresponding value, as assessed by RRBS. MSCC, compared to RRBS, somewhat underestimates the degree of hypermethylation for many genes. Thus, if anything, the number of genes aberrantly downregulated by promoter hypermethylation was underestimated by the MSCC approach.

Figure S5



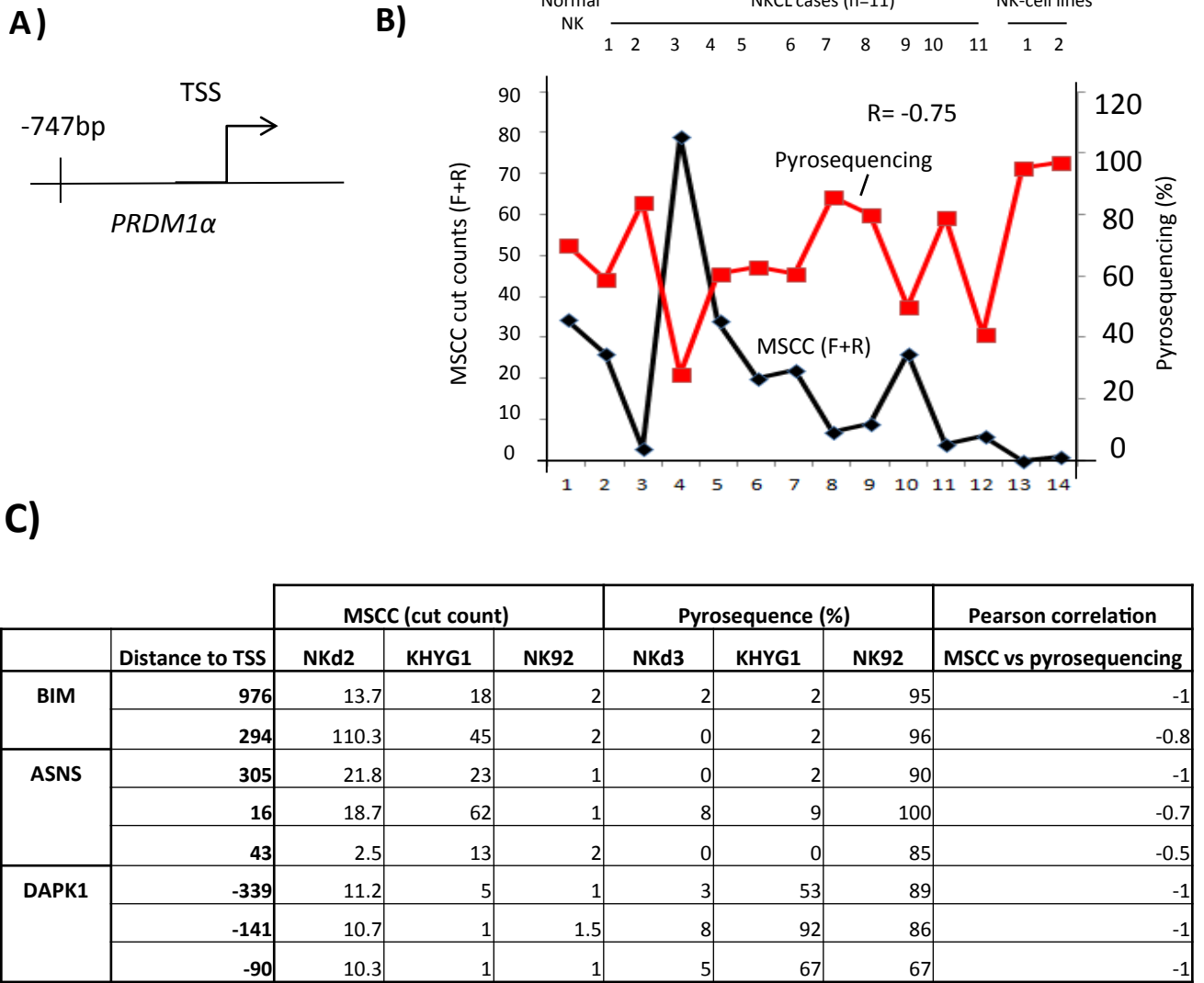
Hypermethylated candidate tumor suppressor genes have low expression in malignant NK-cell lines. mRNA expression of candidate tumor suppressor genes with promoter methylation was determined with q-RT-PCR in NK-cell lines (n= 6). The mRNA expression for pro-apoptotic genes *BIM* and *DAPK1* (A), JAK-STAT signaling pathway genes, *SOCS6*, *IL12RB2* and *ZFH3* (B), *TET2* and *TLE1* (C), *ASNS* and *CD300A* (D) were evaluated with q-RT-PCR in NK-cell lines. Normal resting or 48h IL2-activated NK cells served as controls. Expression values were calibrated to the expression levels in resting NK cells. The housekeeping gene *RPL13A* was used for normalization of gene expression. Hypermethylation status of each gene is shown below each plot based on the MSCC results in two NK-cell lines. A (+) sign indicates >1 log2 reduction in the average promoter cut count (i.e. ±1 kb of the TSS) in the NK-cell line compared to the average promoter cut count of 48h IL2-activated NK cells (n=3). A (-) sign indicates no hypermethylation. Hypermethylation status of *BIM*, *DAPK1* and *ASNS* promoters are indicated for two NK-cell lines (NK92, KHYG1) and activated PB NK cells based on pyrosequencing results. (+): Methylated, (-): No methylation. The level of promoter methylation of each gene is indicated based on q-MSP results in NK-cell lines and represented as methylation change compared to 3 day IL2-activated normal NK cells (NKd3). (-): no methylation; (+): hypermethylated; (++) : highly hypermethylated. NA: Not available. The cut-offs for q-MSP methylation levels are as follows for *BIM* and *ASNS*: (-): X<4; (+): 4<X<8; (++) : X>8, where X= dCt (NK-cell line - NKd3)U - dCt(NK-cell line - NKd3)M. Hypermethylation of the four or three genes evaluated respectively with only unmethylated or methylated DNA specific primers are determined as follows: (-): -2.5<Y< 2.5; (+): 2.5<Y<5; (++) : Y>5, where Y= dCt (NK-cell line - NKd3)U or = -(NK-cell line - NKd3)M. NKd3 methylation level was determined to be negative for all genes after comparing amplification of it to unmethylated or methylated control DNAs [ΔCt(NKd3-unmethylated control DNA) <2 for unmethylated DNA specific primers ; no amplification of NKd3 was observed with methylated DNA specific primers]. R: Resting NK cells; A: 48h IL2-activated NK cells; NA: Not available. *: *ASNS* mRNA expression in KHYG1 cell line.

Figure S6



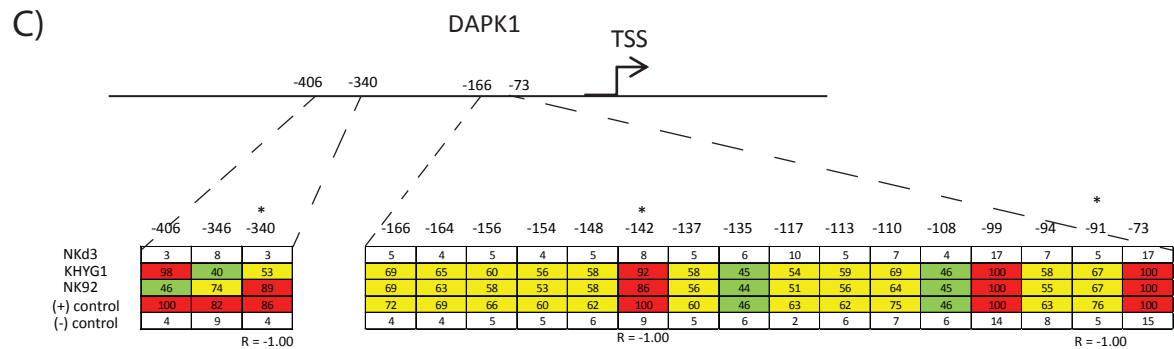
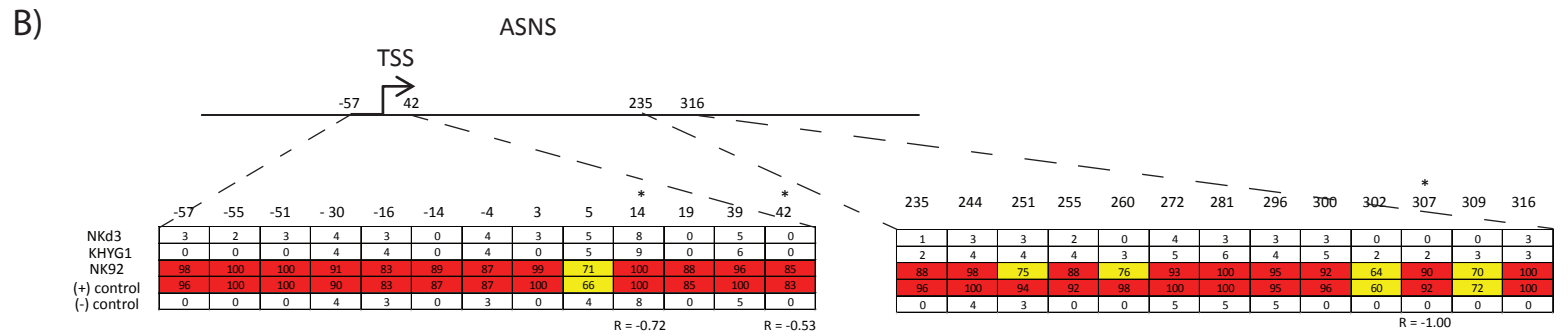
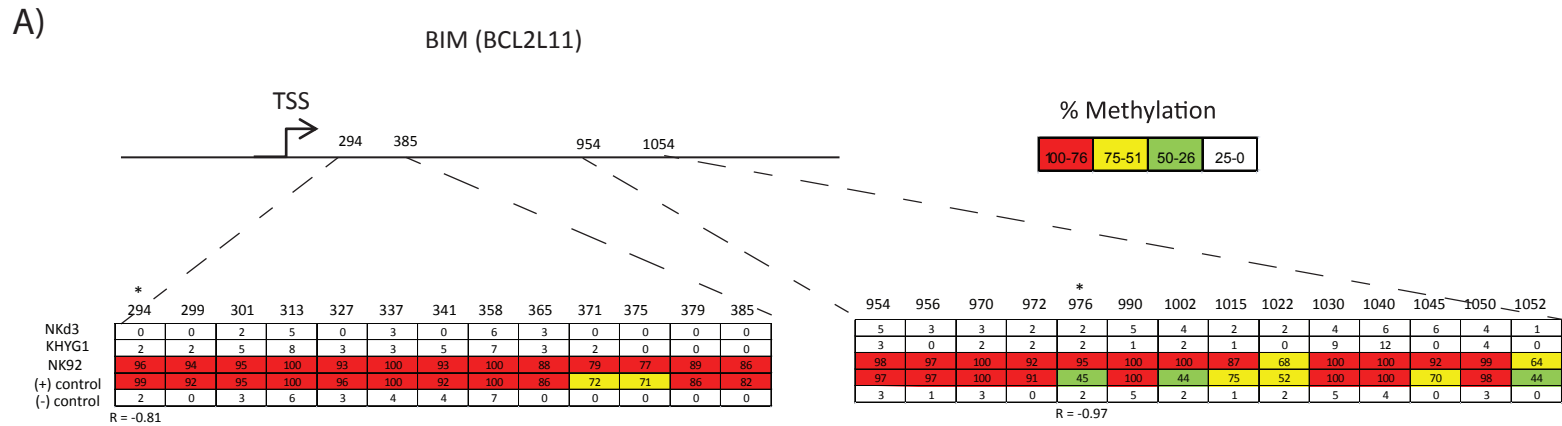
BIM protein is silenced in NK-cell lines. BIM protein expression is evaluated with western blotting using 6 NK-cell lines. 3 day IL2-activated PB NK cells (NKd3) and BIM-EL-transfected 293T cells were used as controls. α -tubulin was used as the loading control. The figure shows results from a representative experiment that was repeated three times.

Figure S7



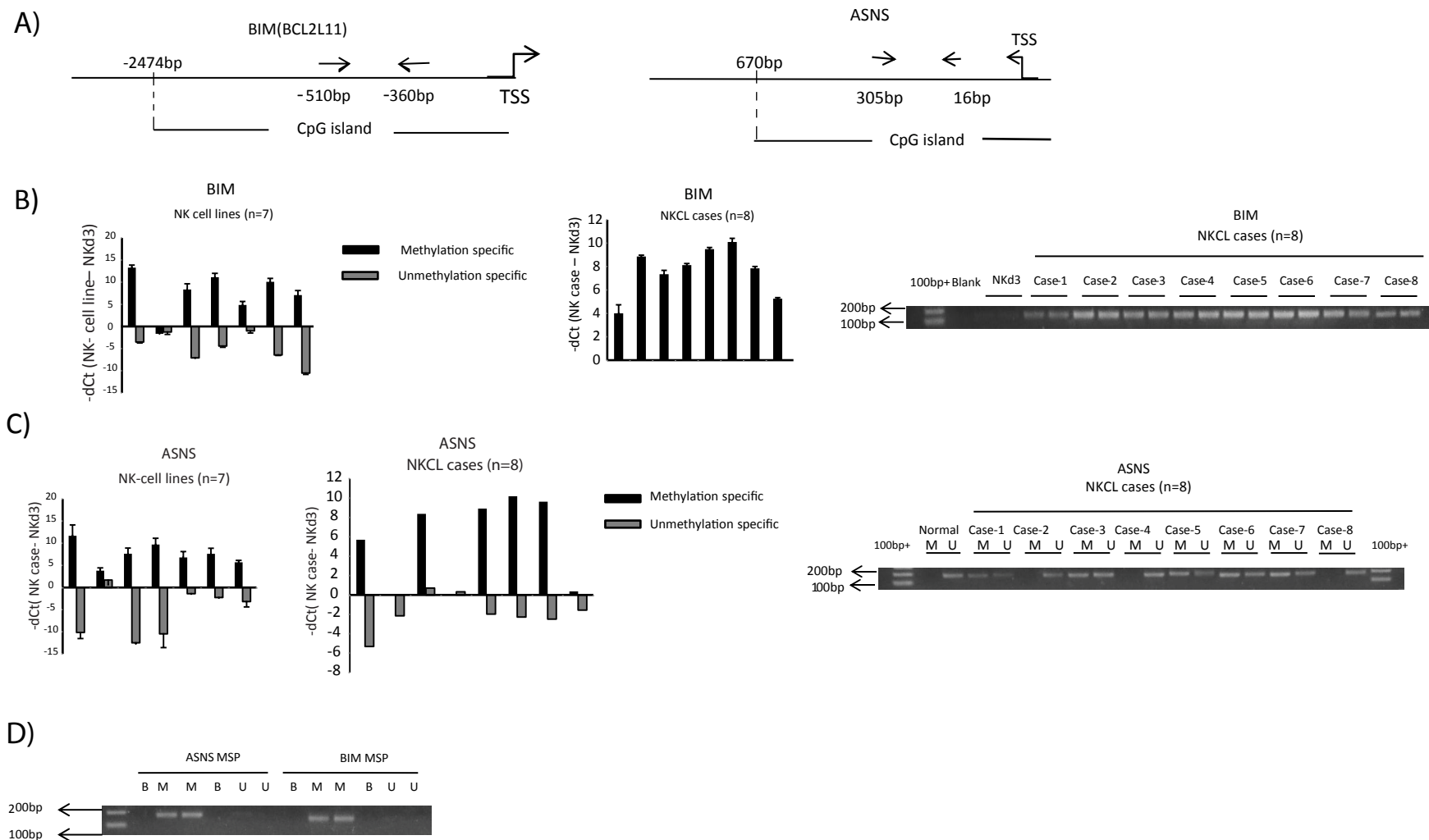
Comparison of MSCC with locus-specific pyrosequencing. (A) MSCC and biotage pyrosequencing data were both available only for -747 bp from the PRDM1 α TSS in 13 malignant NK samples (11 NKCL cases and two NK-cell lines). (B) The relationship between MSCC cut counts and the percent methylation based on pyrosequencing were compared between each malignant NK sample and the average of normal NK cells. MSCC cut counts originating from F and R strands are summed for each NK sample. Pearson correlation (R) is shown above the plot. (C) Numeric values show the cut count number (MSCC) and % methylation (pyrosequencing) for each HpaII site having both MSCC and pyrosequencing data available in *BIM*, *DAPK1*, and *ASNS* promoters for KHYG1 and NK92 cell lines and NK-cells (NKd3, pyrosequencing; NKd2, MSCC).

Figure S8



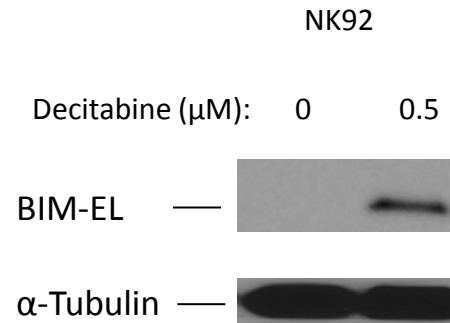
Pyrosequencing analysis of *BIM*, *ASNS* and *DAPK1* promoters in NK-cell lines and normal NK-cells cross-validates MSCC results. Heatmaps show the percentage methylation level in all available CpG sites in two separate locations \pm 1kb of TSS of *BIM* (A), *ASNS* (B) and *DAPK1* (C) in two NK-cell lines with MSCC data (i.e. KHYG1 and NK92) and 3 day activated NK cells (i.e. NKd3). *: The CpG sites at which both MSCC and pyrosequencing data available. R values below these CpG sites show the Pearson correlation of MSCC cut count number and the percentage methylation based on pyrosequencing. The numbers in each box show the percentage methylation for the specific CpG site and the sample. The color scale in bottom right shows % methylation range for each color. (+) Control: Methylated control; (-) Control: Unmethylated control samples as described in Supplementary Methods.

Figure S9



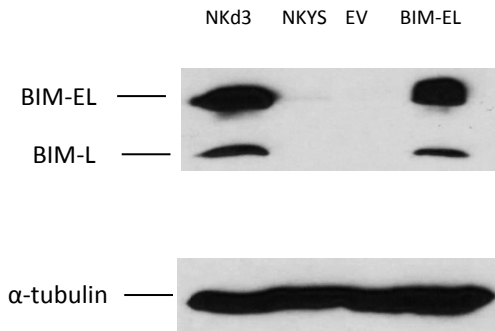
Validation of *BIM* and *ASNS* promoter methylation with locus-specific q-MSP in malignant NK samples. (A) The loci evaluated by q-MSP near the *BIM* (left) and *ASNS* (right) TSSs are shown with arrows based on the UCSC genome browser. The locations of the CpG islands around the TSSs are indicated. (B) Ct value difference between 3 day IL2-activated NK cells and NK-cell lines (left) or 8 NKCL cases (middle) during logarithmic amplification phase of q-PCR using methylated or unmethylated DNA specific BIM MSP primers are shown. Result is shown from agarose gel electrophoresis of q-MSP products using methylated DNA specific BIM primers in NKCL cases (right). Panel C provide data for ASNS corresponding to panel B above. (D) Agarose-gel electrophoresis showing the q-MSP products of methylated or unmethylated DNA specific primers using M.SssI methylated human genomic DNA. M represents methylated DNA specific, U represents unmethylated DNA specific q-MSP primers. Data are shown as mean \pm SD of two independent experiments. NKd3: 3 day IL2 activated peripheral blood NK cells. If $[dCt(NKd3 - malignant NK sample)]_M - [dCt(NKd3 - malignant NK sample)]_U > 4$, then the sample was considered hypermethylated.

Figure S10



BIM protein is induced after Decitabine treatment. BIM-EL protein expression is evaluated after treatment of NK92 cells with 0.5 μM of Decitabine for 4 days as described in Materials and Methods. The result is representative of two experiments.

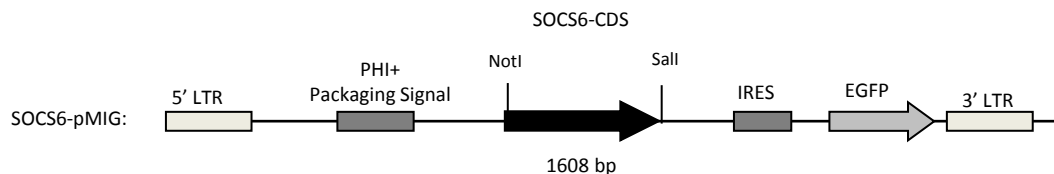
Figure S11



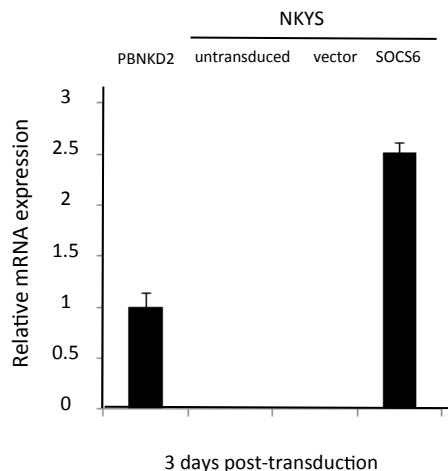
Ectopic expression of BIM in NKYS cells 2 days post-transduction. Ectopic expression of *BIM* in BIM-EL transduced, unsorted NKYS cells was shown with western blot 2 days post-transduction. NK cells activated with IL2 for 3 days were used as the positive control. Untransduced and empty vector (EV) transduced NKYS cells were used as negative controls. α -tubulin was used as the loading control. NKd3: 3 day IL2 activated PB NK cells.

Figure S12

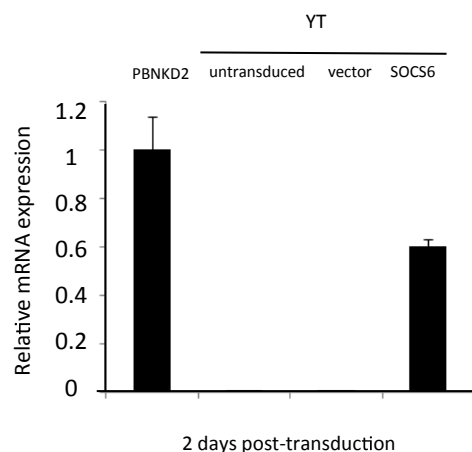
A)



B)



C)



Ectopic expression of SOCS6 in NK-cell lines. (A) The retroviral construct used in the reconstitution of SOCS6. (B) q-RT-PCR was applied on untransduced NKYS cells, empty vector (EV) or SOCS6-transduced NKYS cells 3 days post-transduction. (C) q-RT-PCR was applied on untransduced YT cells, empty vector or SOCS6 transduced YT cells 2 days post-transduction. Unsorted cells were used for q-RT-PCR. RPL13A mRNA expression was used to normalize SOCS6 expression in each sample. SOCS6 expression in empty vector transduced NK-cell lines were used for comparison of the SOCS6 mRNA expression. Data show means (+/- SD). NKd2: 2 day IL2 activated NK cells.